High Temperature Free Radical Polymerization. 2. Modeling Continuous Styrene Polymerization

J. D. Campbell

Johnson Polymer, Innovatielaan 1, NL-8440 AJ, Heerenveen, The Netherlands

F. Teymour

Department of Chemical Engineering, Illinois Institute of Technology, Chicago, Illinois 60616

M. Morbidelli*

Swiss Federal Institute of Technology Zurich, Laboratorium für Techniche Chemie/LTC, ETH−Hönggerberg/HCl, CH-8093 Zurich, Switzerland

Received April 25, 2002; Revised Manuscript Received March 27, 2003

ABSTRACT: A comprehensive kinetic model for the thermal polymerization of styrene at temperature values between 250 and 350 °C, capable of calculating monomer kinetics, oligomer concentrations, and molecular weight and terminal double bond (TDB) distributions, is described. The model, based on the mechanism described in the first part of this work (*Macromolecules* **2003**, *36*, 0000), accounts for polymerization, thermal initiation, and degradation reactions, including backbiting, chain transfer to polymer, and addition to terminal unsaturation, all followed by β-scission. All activation energies for the rate parameters were taken from independent literature sources, with the exception of backbiting for which the experimental data obtained in part 1 of this work have been used. The frequency factors for the backbiting, chain transfer to polymer, and addition fragmentation reactions were fitted using a combination of molecular weight, oligomer concentration, and terminal double bond distribution (TDB) data for three different temperature values. Using these parameter values, the model was found to adequately predict the oligomer concentrations, molecular weights, and TDB distributions over the entire range of experimental conditions examined in the first part of this work. The kinetic model indicates that this polymerization is characterized and controlled by aggressive backbiting, followed by β-scission degradation.

Introduction

As discussed in the first part of this work,[1] the thermally initiated polymerization of styrene at temperatures above 250 °C is characterized by fast reaction kinetics, low molecular weights and significant levels of low molecular weight oligomers. In this temperature range, thermal initiation, propagation, chain transfer, and polymer degradation reactions contribute to the complex polymerization mechanism. A great deal of work has been reported in the literature on the mechanism of thermal initiation and degradation reactions, which have been mostly studied separately and in the absence of polymerization. Such a wealth of literature information, along with our own mechanistic studies,[1,2] is discussed in the first part of this work with the aim of proposing a comprehensive mechanism for this polymerization. In this paper, we present a kinetic model that reflects this mechanism, and we validate it by comparison with a broad range of experimental data. These data refer to CSTR experiments and include monomer conversion, molecular weight averages and distributions, terminal double bond (TDB) distributions and specific oligomer concentrations as a function of temperature and residence time, as reported in detail in Table 1 in part 1 of this work.[1]

The pioneering attempts to quantitatively model this system were made by Hui and Hamielec[3] and Husain and Hamielec.[4] In these works, the kinetics of the thermal initiation reaction was studied between 100 and 230 °C and found to be third order in monomer concentration, consistent with the mechanism initially proposed by Mayo.[5] The developed model was able to successfully simulate the monomer kinetics in this temperature range. The molecular weight modeling was less successful, however, requiring the introduction of empirical relationships.

Subsequent work of Hamielec et al.[6] showed that the model of Hui and Hamielec[3] when extended to styrene/acrylic acid copolymers was capable of describing the monomer kinetics up to 300 °C in a CSTR, while the molecular weight predictions were unsatisfactory. Low molecular weight oligomers, specifically dimers and trimers, were identified by gas chromatography and shown to increase with increasing residence time and temperature. However, these species were not included in the kinetic model.

With the above notable exceptions, there have been no attempts to model the kinetics of this polymerization system. Nonetheless, there are examples of models that describe the degradation of polymers, which is an important component of this system. Ziff and McGrady[7] presented a model for polymer degradation using a continuous molecular weight variable, to describe fragmentation in various positions in the chain. A similar modeling approach was used by Wang et al.[8] to describe the degradation of poly(stryene−allyl alcohol). They proposed a mechanism that included random and specific chain scission, the latter producing low molecular weight oligomers. Kodera and McCoy[9] proposed a similar but more comprehensive model, also based on a continuous distribution, and accounted for addition reactions. Similar modeling approaches[10−13] have been

* Corresponding author.

10.1021/ma020643u CCC: $25.00
Published on Web 06/25/2003

applied to the degradation of a variety of polymers. Woo and Broadbelt[14] and Kruse et al.[15] used a more comprehensive modeling scheme to describe the degradation of polystyrene, based on a reaction generating algorithm. The extremely large number of reactions however makes it computationally difficult for this approach to be used for high molecular weight polymers. Kinetic rate constants for each reaction generated were estimated using the Evans−Polanyi[16] relationship and an online heat of reaction database.

Model Equations

The objective of the model presented here is to simulate the molecular weight distribution, oligomer concentrations, and terminal double bond distribution for the thermal polymerization of styrene at temperatures above 250 °C. The population balance approach has been used in order to describe the above distributions. Because of the low molecular weight of the polymers under consideration, it has been possible to model individually each chain length in the population without introducing any discretization technique. The steady-state model was solved using the direct substitution method. For extreme parameter values (for example 2 or 3 orders of magnitude larger than the standard parameter set) for the reactions that involve reinitiation of dead polymer chains, such as addition/fragmentation and chain transfer to polymer, some convergence difficulties have been found. In these cases, the full dynamic model was used, and the steady state was computed at the end of the transient, however at a substantial increase of computational cost.

As described in the first paper in this series, the reaction mechanism is a complex combination of typical free radical polymerization reactions (propagation, termination, chain transfer), thermal initiation, and polymer degradation. We have shown that the degradation reactions dominate the molecular weight development of this polymerization. Specifically, backbiting followed by β-scission is the dominant chain producing mechanism, although there are contributions to molecular weight development from chain transfer to polymer (CTP) and addition fragmentation (AF). All these chain degradation reactions are included in the model.

Each hydrogen abstraction reaction produces a midchain radical intermediate that we assume does not propagate or terminate by combination to any appreciable extent so that branching is not considered in the model. This assumption is based on a detailed NMR investigation, discussed in detail elsewhere,[2] which demonstrates that the concentration of quaternary carbons on the polymer chains, indicative of branch points, is negligible. The midchain radical undergoes β-scission, producing two smaller fragments, a radical and a polymer chain with a terminal double bond (TDB). Since all chains are linear, polymer chains have the possibility of having 0, 1, or 2 TDBs, while radicals can have only 0 or 1 TDB, since a radical center exists on the chain end. Consequently, we consider in the following population balances for polymer and radical chains subdivided based on these end groups, that is $P_{r,a}$ and $R_{r,a}$ where "r" represents the number of monomer units in the chain and "a" the number of terminal double bonds. The backbiting/β-scission reactions (1:3, 1:5 or 1:7 transfer) produce dead oligomers P_i^* of length $i = 2$, 3, or 4 with one TDB or oligomeric radicals R_i^* of length $i = 1$, 2 or 3, respectively. For the sake of clarity, we compute these species through separate mass balances which are discussed in detail in the following paragraphs.

Obviously, when computing the overall weight fraction, $w_{P^*_i}$, of an oligomer containing "i" monomers, we have to include the corresponding species computed in the two sets of mass balances, so that

$$w_{P^*_i} = \frac{(P_i^* + P_{i,0} + P_{i,1} + P_{i,2})i}{Q_1} \tag{1}$$

where Q_1 is the first moment of the overall polymer distribution, which can be approximated by

$$Q_1 = \sum_{r=2}^{N}(P_{r,0} + P_{r,1} + P_{r,2})r + \sum_{i=2}^{4} P_i^* i \tag{2}$$

where N is the maximum chain length used in the calculation. This value is selected for each simulation so that all moments converge; that is, chains with longer length are not present to any meaningful extent.

The reaction mechanisms relevant to this polymerization have been identified in Figure 1, parts a−g, in part 1 of this series.[1] From this kinetic scheme, the population balances for the radical and polymer species for each chain length and terminal double bond end group are derived. To do this, we used the reaction kinetics summarized in Tables 1 and 2 for the production and consumption of each radical and polymer species, respectively.

Radical Population Balance. All reactions that consume and produce radicals of chain length "r" with "a" TDBs, denoted $R_{r,a}$, where "a" can be 0 or 1, are accounted for in the model. These radicals are consumed by the propagation, termination, chain transfer to polymer, backbiting and chain end β-scission (depropagation) reactions listed in the upper part of Table 1. In the case of backbiting, the 1:3, the 1:5, and the 1:7 hydrogen transfer reactions are possible, whose rate constants are denoted by k_{B1}, k_{B2}, and k_{B3}, respectively. These reactions produce a midchain radical located at a specific location on the chain, denoted with a superscript representing the carbon that has the radical center, i.e., $R_{r,a}^{-3}$, $R_{r,a}^{-5}$, or $R_{r,a}^{-7}$. These midchain radicals can abstract a hydrogen from the chain end due to the proximity and favored configuration of the chain end with respect to the midchain. The rate constants for these reverse hydrogen abstraction reactions are k_{-B1}, k_{-B2}, and k_{-B3} for the 1:3, 1:5, and 1:7 backbiting reactions, respectively. It is important to note that a radical must be of a minimum length for backbiting to be possible. For example, a radical must contain at least three monomer units for the 1:3 backbiting reaction, four units for the 1:5 reaction, and five units for the 1:7 transfer to be possible. These restrictions are accounted for in the population balance. Chain end β-scission, equivalent to depropagation, can also occur when a radical, of length greater than one unit, is on the chain end and a monomer unit cleaves from the growing radical. The rate constant for this reaction is denoted $k_{\beta SE}$. A growing radical can also react with a TDB on a polymer chain, $P_{s,a}$ or polymeric oligomer, P_i^* (where the length "i" equals 2, 3 or 4) by addition, producing a midchain radical, denoted $R_{s,a}^{\oplus}$. This radical can undergo β-scission in one of the two possible β positions, whose rate constants are denoted by $k_{\beta S1}$ or $k_{\beta S2}$. Note

Table 1. Reactions that Produce and Consume the Radicals, $R_{r,a}$ with "*r*" Monomer Units and "*a*" Terminal Double Bonds, and the Oligomeric Radicals, R_i^*, with $i = 1, 2, 3$

Consumption of $R_{r,a}$

addition, abstraction and termination reactions

$$R_{r,a} + M \xrightarrow{k_p} R_{r+1,a}$$

$$R_{r,a} + P_{s,b} \xrightarrow{k_{fp}} R^{\oplus}_{s,b} + P_{r,a}$$

$$R_{r,a} + P^*_i \xrightarrow{k_{fp}} R^{\oplus}_{i,1} + P_{r,a}$$

$$R_{r,a} + R_{s,b} \xrightarrow{k_{tc}} P_{r+s,a+b}$$

$$R_{r,a} + R_{s,b} \xrightarrow{k_{td}} P_{s,b} + P_{r,a}$$

addition fragmentation

$$R_{r,a} + P_{s,b>0} \underset{k_{\beta S1}}{\overset{k_{AF}}{\rightleftharpoons}} R^{\oplus}_{r+s,a+b-1}$$

$$R_{r,a} + P^*_i \underset{k_{\beta S1}}{\overset{k_{AF}}{\rightleftharpoons}} R^{\oplus}_{r+i,a}; \quad i = 2, 3, 4$$

backbiting

$$R_{r,a} \underset{k_{-B1}}{\overset{k_{B1}}{\rightleftharpoons}} R^{-3}_{r,a}, \quad \text{for } r \geq 3$$

$$R_{r,a} \underset{k_{-B2}}{\overset{k_{B2}}{\rightleftharpoons}} R^{-5}_{r,a}, \quad \text{for } r \geq 4$$

$$R_{r,a} \underset{k_{-B3}}{\overset{k_{B3}}{\rightleftharpoons}} R^{-7}_{r,a}, \quad \text{for } r \geq 5$$

chain end β-scission

$$R_{r,a} \xrightarrow{k_{\beta SE}} R_{r-1,a} + M, \quad \text{for } r \geq 2$$

Production of $R_{r,a}$

backbiting/β-scission

1,3 hydrogen transfer

$$R_{r+2,a} \underset{k_{-B1}}{\overset{k_{B1}}{\rightleftharpoons}} R^{-3}_{r+2,a} \xrightarrow{k_{\beta S1}} R_{r,a} + P^*_2$$

$$\xrightarrow{k_{\beta S2}} R^*_1 + P_{r+1,a+1}$$

1,5 hydrogen transfer

$$R_{r+3,a} \underset{k_{-B2}}{\overset{k_{B2}}{\rightleftharpoons}} R^{-5}_{r+3,a} \xrightarrow{k_{\beta S1}} R_{r,a} + P^*_3$$

$$\xrightarrow{k_{\beta S2}} R^*_2 + P_{r+1,a+1}$$

1,7 hydrogen transfer

$$R_{r+4,a} \underset{k_{-B3}}{\overset{k_{B3}}{\rightleftharpoons}} R^{-7}_{r+4,a} \xrightarrow{k_{\beta S1}} R_{r,a} + P^*_4$$

$$\xrightarrow{k_{\beta S2}} R^*_3 + P_{r+1,a+1}$$

addition/β-scission

$$R_{s,a} + P_{r+1,b>0} \underset{k_{\beta S1}}{\overset{k_{AF}}{\rightleftharpoons}} R^{\oplus}_{r+s+1,a+b-1} \xrightarrow{k_{\beta S2}} R_{r,b-1} + P_{s+1,a+1}$$

$$R_{s,a} + P^*_i \underset{k_{\beta S1}}{\overset{k_{AF}}{\rightleftharpoons}} R^{-(2i-1)}_{s+i,a} \xrightarrow{k_{\beta S2}} R^*_{i-1} + P_{s+1,a+1}$$

CTP/β-scission

$$R_{n,a} + P_{r+s,b} \xrightarrow{k_{fp}} R^{\oplus}_{r+s,b} + P_{n,a}$$

for $b = 0$

$$R^{\oplus}_{r+s,0} \xrightarrow{k_{\beta S1}} R_{r,0} + P_{s,1}$$

$$\xrightarrow{k_{\beta S2}} R_{s,0} + P_{r,1}$$

for $b = 1$

$$R^{\oplus}_{r+s,1} \xrightarrow{k_{\beta S1}} R_{r,0} + P_{s,2}$$

$$\xrightarrow{k_{\beta S2}} R_{s,1} + P_{r,1}$$

or

$$R^{\oplus}_{r+s,1} \xrightarrow{k_{\beta S1}} R_{r,1} + P_{s,1}$$

$$\xrightarrow{k_{\beta S2}} R_{s,0} + P_{r,2}$$

for $b = 2$

$$R^{\oplus}_{r+s,2} \xrightarrow{k_{\beta S1}} R_{r,1} + P_{s,2}$$

$$\xrightarrow{k_{\beta S2}} P_{r,2} + R_{s,1}$$

addition

$$R_{r-1,a} + M \xrightarrow{k_p} R_{r,a}$$

chain end β-scission

$$R_{r+1,a} \xrightarrow{k_{\beta SE}} R_{r,a} + M, \quad \text{for } r \geq 1$$

that the possibility of addition to internal terminal unsaturation moieties formed by disproportionation has been neglected due to their low concentration and low reactivity compared to the vinylic terminal unsaturations formed by β-scission.

The reactions capable of producing radical chains with "*r*" monomer units and "*a*" TDBs are listed in the lower part of Table 1. The backbiting reaction produces a midchain radical in either the third, fifth, or seventh carbon from the chain end, which can break in one of the two possible "β" positions, denoted by $k_{\beta S1}$ or $k_{\beta S2}$. In the case of $k_{\beta S1}$, an oligomeric polymer chain, P^*_i with a TDB is formed, and the radical remains on the larger fragment. Therefore, a radical of length "*r*" is formed from a larger radical of length "*r*+*i*", where "*i*" is the length of the oligomer. Alternatively, the chain can break in the "$k_{\beta S2}$" position, resulting in an oligomeric radical, P^*_i and a larger dead polymer chain with at least one TDB. Chain transfer to polymer produces a midchain radical at a random position in the chain, denoted $R^{\oplus}_{r+s,b}$. Since the original polymer can have 0, 1, or 2 TDBs, and the midchain radical could break in either one of the two "β" positions, the number of TDBs on the resulting radical fragments can be accounted for explicitly, as shown in Table 1. The probability (α) that the chain breaks in the $k_{\beta S1}$ position is given by

$$\alpha = \frac{k_{\beta S1}}{k_{\beta S1} + k_{\beta S2}} \tag{3}$$

Since it is unlikely that the rate constant $k_{\beta S1}$ or $k_{\beta S2}$ are different, especially for chains whose radical is far from the chain end, we have assumed $\alpha = {}^1/_2$, that is an equal probability that the chain breaks in either of the two positions. Note that the backbiting reaction followed by β-scission is treated as a lumped reaction. Since it has been found that β-scission is the rate-determining step, the overall kinetics has been de-

Table 2. Reactions that Produce and Consume the polymer Chains $P_{r,a}$ of Length "*r*" with "*a*" TDBs, and the polymeric Oligomers P_i^*, with $i = 2, 3, 4$

Consumption of $P_{r,a}$

CTP

$$P_{r,a} + R_{s,b} \xrightarrow{k_{fp}} R_{r,a}^{\oplus} + P_{s,b}$$

addition fragmentation

$$P_{r,a>0} + R_{s,b} \underset{k_{\beta S1}}{\overset{k_{AF}}{\rightleftharpoons}} R_{r+s,a+b-1}^{\oplus}$$

Production of $P_{r,a}$

CTP

$$R_{r,a} + P_{s,b} \xrightarrow{k_{fp}} R_{s,b}^{\oplus} + P_{r,a}$$

$$R_{r,a} + P_i^* \xrightarrow{k_{fp}} R_{i,1}^{\oplus} + P_{r,a}; \quad i = 2, 3, 4$$

backbiting/β-scission

1,3 hydrogen transfer

$$R_{r+1,a-1} \underset{k_{-B1}}{\overset{k_{B1}}{\rightleftharpoons}} R_{r+1,a-1}^{-3} \xrightarrow{k_{\beta S1}} R_{r-1,a-1} + P_2^* \quad r>1$$

$$\xrightarrow{k_{\beta S2}} R_1^* + P_{r,a}$$

1,5 hydrogen transfer

$$R_{r+2,a-1} \underset{k_{-B2}}{\overset{k_{B2}}{\rightleftharpoons}} R_{r+2,a-1}^{-5} \xrightarrow{k_{\beta S1}} R_{r-1,a-1} + P_3^* \quad r>1$$

$$\xrightarrow{k_{\beta S2}} R_2^* + P_{r,a}$$

1,7 hydrogen transfer

$$R_{r+3,a-1} \underset{k_{-B3}}{\overset{k_{B3}}{\rightleftharpoons}} R_{r+3,a-1}^{-7} \xrightarrow{k_{\beta S1}} R_{r-1,a-1} + P_4^* \quad r>1$$

$$\xrightarrow{k_{\beta S2}} R_3^* + P_{r,a}$$

addition/β-scission

$$R_{r-1,a-1} + P_{s,b>0} \underset{k_{\beta S1}}{\overset{k_{AF}}{\rightleftharpoons}} R_{r+s-1,a+b-2}^{\oplus} \xrightarrow{k_{\beta S2}} R_{s-1,b-1} + P_{r,a}$$

$$R_{r-1,a-1} + P_i^* \underset{k_{\beta S1}}{\overset{k_{AF}}{\rightleftharpoons}} R_{r+i-1,a-2}^{-(2i-1)} \xrightarrow{k_{\beta S2}} R_{r-i,0} + P_{r,a}$$

bimolecular termination

$$R_{s,k} + R_{r-s,a-k} \xrightarrow{k_{tc}} P_{r,a}$$

$$R_{r,a} + R_{s,b} \xrightarrow{k_{td}} P_{s,b} + P_{r,a}$$

CTP/β-scission

$$R_{n,j} + P_{r+s,b} \xrightarrow{k_{fp}} R_{r+s,b}^{\oplus} + P_{n,j}$$

for $b = 0$

$$R_{r+s,0}^{\oplus} \xrightarrow{k_{\beta S1}} R_{r,0} + P_{s,1}$$

$$\xrightarrow{k_{\beta S2}} P_{r,1} + R_{s,0}$$

for $b = 1$

$$R_{r+s,1}^{\oplus} \xrightarrow{k_{\beta S1}} R_{r,0} + P_{s,2}$$

$$\xrightarrow{k_{\beta S2}} P_{r,1} + R_{s,1}$$

or

$$R_{r+s,1}^{\oplus} \xrightarrow{k_{\beta S1}} R_{r,1} + P_{s,1}$$

$$\xrightarrow{k_{\beta S2}} P_{r,2} + R_{s,0}$$

for $b = 2$

$$R_{r+s,2}^{\oplus} \xrightarrow{k_{\beta S1}} R_{r,1} + P_{s,2}$$

$$\xrightarrow{k_{\beta S2}} P_{r,2} + R_{s,1}$$

scribed using the lumped rate constant, defined in part 1[1] as follows:

$$k'_{Bi} = \frac{k_{\beta S} k_{Bi}}{k_{-Bi}} \quad \text{for } i = 1, 2 \text{ or } 3 \tag{4}$$

where $k_{\beta S} = k_{\beta S1} + k_{\beta S2}$, reflecting the overall β-scission rate constant.

Using the reaction scheme shown in Table 1 the population balance for radical chains, $R_{r,a}$ containing "*r*" monomer units and "*a*" terminal double bonds has been derived, as shown below. The oligomeric radicals, R_i^* formed by the backbiting/β-scission reaction via "$k_{\beta S2}$", are treated separately in the next section. Given the following definitions

$$\tau = \frac{k_{td} Y_0}{k_p[M]}; \quad \beta = \frac{k_{tc} Y_0}{k_p[M]}; \quad C_{AF} = \frac{k_{AF}}{k_p[M]}$$

$$C_B = \frac{\sum_{i=1}^{3} k'_{Bi}}{k_p[M]}; \quad C_s = \frac{k_{\beta SE}}{k_p[M]}; \quad C_{fp} = \frac{k_{fp}}{k_p[M]}$$

while using the quasi steady-state approximation (QSSA), and neglecting radical outflow, we obtain for r≥1:

$$R_{r,0} = \left\{ R_{r-1,0} + \delta(r-4) R_3^* + \frac{\alpha}{k_p[M]} \sum_{i=1}^{3} k'_{Bi} R_{r+i+1,0} + \delta (r-1) \frac{R_I}{k_p[M]} + (1-\alpha) C_{AF} Y_0 P_{r+1,1} + C_s R_{r+1,0} + C_{fp} Y_0 \left\{ \sum_{s=2}^{\infty} P_{r+s,0} + \frac{1}{2} \sum_{s=2}^{\infty} (P_{r+s,1} + P^*_{r+s}) \right\} \right\} \Big/ \left[1 + \tau + \beta + C_{fp} \{ \sum_{i=0}^{2} (Q_{1,i} - 2Q_{0,i}) + \sum_{i=2}^{4} (i-2) P_i^* \} + \delta(r>1) C_s + \sum_{i=1}^{3} \delta(r > i+1) \frac{k'_{Bi}}{k_p[M]} + (1-\alpha) C_{AF} \left(\sum_{i=1}^{2} i Q_{0,i} + \sum_{i=2}^{4} P_i^* \right) \right] \tag{5}$$

$$R_{r,1} = \left\{ R_{r-1,1} + \frac{\alpha}{k_p[M]} \sum_{i=1}^{3} k'_{Bi} R_{r+i+1,1} + 2(1-\alpha) C_{AF} Y_0 P_{r+1,2} + C_s R_{r+1,1} + C_{fp} Y_0 \left\{ \sum_{s=2}^{\infty} P_{r+s,2} + \frac{1}{2} \left(\sum_{s=2}^{\infty} (P_{r+s,1} + P^*_{r+s}) \right) \right\} \right\} \Big/ \left[1 + \tau + \beta + C_{fp} \{ \sum_{i=0}^{2} (Q_{1,i} - 2Q_{0,i}) + \sum_{i=2}^{4} (i-2) P_i^* \} + \delta(r>1) C_s + \sum_{i=1}^{3} \delta(r > i+1) \frac{k'_{Bi}}{k_p[M]} + (1-\alpha) C_{AF} \left(\sum_{i=1}^{2} i Q_{0,i} + \sum_{i=2}^{4} P_i^* \right) \right] \tag{6}$$

where R_I is the rate of initiation given by eq 1 in part 1, $\delta(r > i)$ is a function equal to zero for $r \leq i$ and to 1 for $r > i$, and $\delta(r > i)$ is another function equal to 1 for $r = i$ and to zero for $r \neq i$.

Note that in the terms relating to backbiting, it has been considered that a radical chain must contain at least three monomer units for the 1:3 transfer to be possible, four units for the 1:5 transfer, and five units for the 1:7 transfer. This correction becomes particularly important at the highest temperature conditions where the average degree of polymerization can be as low as 10. In these cases, the fraction of the total radical population that is too short to backbite becomes significant.

Oligomeric Radicals. The oligomeric radicals, R_1^*, R_2^* and R_3^*, are produced by the backbiting/β-scission reaction. Specifically, radicals of length 1 are produced from the 1:3 transfer (k'_{B1}), of length 2 from the 1:5 transfer (k'_{B2}) and of length 3 from the 1:7 transfer (k'_{B3}). These and all the other reactions which produce or consume the oligomeric radicals are summarized in Table 2. The corresponding mass balances are given by

$$R_1^* = \left\{(1-\alpha)\left[\frac{k'_{B1}}{k_p[M]}(Y_0 - \sum_{j=1}^{2}(R_{j,0} + R_{j,1} + R_j^*)) + C_{AF}P_2^*Y_0\right] + C_S R_2^*\right\}/\{1 + \tau + \beta + (1-\alpha)C_{AF}(\sum_{i=1}^{2} iQ_{0,i} + \sum_{i=2}^{4} P_i^*) + C_{fp}\{\sum_{i=0}^{2}(Q_{1,i} - 2Q_{0,i}) + \sum_{i=2}^{4}(i-2)\,P_i^*\}\} \quad (7)$$

$$R_2^* = \left\{(1-\alpha)\left[\frac{k'_{B2}}{k_p[M]}(Y_0 - \sum_{j=1}^{3}(R_{j,0} + R_{j,1} + R_j^*)) + C_{AF}P_3^*Y_0\right] + C_S R_3^* + R_1^*\right\}/\{1 + \tau + \beta + (1-\alpha)C_{AF}(\sum_{i=1}^{2} iQ_{0,i} + \sum_{i=2}^{4} P_i^*) + C_{fp}\{\sum_{i=0}^{2}(Q_{1,i} - 2Q_{0,i}) + \sum_{i=2}^{4}(i-2)P_i^*\} + C_S\} \quad (8)$$

$$R_3^* = \left\{(1-\alpha)\left[\frac{k'_{B3}}{k_p[M]}(Y_0 - \sum_{j=1}^{4}(R_{j,0} + R_{j,1} + R_j^*)) + C_{AF}P_4^*Y_0\right] + R_2^*\right\}/\{1 + \tau + \beta + (1-\alpha)C_{AF}(\sum_{i=1}^{2} iQ_{0,i} + \sum_{i=2}^{4} P_i^*) + C_{fp}\{\sum_{i=0}^{2}(Q_{1,i} - 2Q_{0,i}) + \sum_{i=2}^{4}(i-2)\,P_i^*\} + C_S\} \quad (9)$$

The same length restrictions on the backbiting reaction are accounted for in these equations as for the radicals $R_{r,a}$ in eqs 5 and 6.

Polymer Population Balance. All the reactions that consume or produce a polymer chain, $P_{r,a}$ of length "r" with "a" terminal double bonds are summarized in Table 2. Polymer chains can be consumed by chain transfer to polymer or, if the chain has at least one TDB, by addition with a growing radical. In both cases, a midchain radical is produced, $R^{\oplus}_{r,a}$, that undergoes β-scission.

Polymer chains are produced by a variety of polymerization and degradation reactions. Bimolecular termination by either combination or disproportionation produces polymer chains, as does chain transfer to polymer. The 1:3, 1:5, and 1:7 backbiting/β-scission reactions produce midchain radicals, denoted $R^{-3}_{r+1,a-1}$, $R^{-5}_{r+2,a-1}$ or $R^{-7}_{r+3,a-1}$, respectively. If these midchain radicals undergo β-scission via the $k_{\beta S2}$ reaction, a polymer chain of length "r" and an oligomeric radical, R_1^*, R_2^*, or R_3^*, depending on the specific backbiting reaction, are produced. Chain transfer to polymer followed by β-scission can also produce polymer chains. When a hydrogen is abstracted randomly from a polymer chain, a midchain radical ($R^{\oplus}_{r+s,b}$) is produced that can fragment by either the "$k_{\beta S1}$" or the "$k_{\beta S2}$" reaction. The produced smaller polymer fragment has a number of TDBs that depends on the number of TDBs on the original polymer chain, as shown in Table 2. A TDB on a dead polymer chain ($P_{s,b>0}$) can undergo addition with a growing radical ($R_{r-1,a-1}$), producing a midchain radical ($R^{\oplus}_{r+s-1,a+b-2}$). If this chain breaks via the $k_{\beta S2}$ reaction, a polymer chain, one monomer unit longer than the original radical, is generated. If the midchain radical breaks via $k_{\beta S1}$, the original radical and polymer chain are recovered.

On the basis of the kinetic scheme reported in Table 2, the population balances for the polymer chains with chain length "r" and 0, 1, or 2 TDBs, for a CSTR with residence time θ operating under transient conditions, are given by

$$\frac{dP_{r,0}}{dt} = -P_{r,0}\left(\frac{1}{\theta} + (r-2)k_{fp}Y_0\right) + k_{td}(R_{r,0} + R_r^*)Y_0 + \frac{k_{tc}}{2}[\sum_{s<r}(R_{s,0} + R_s^*)(R_{r-s,0} + R_{r-s}^*)] + k_{fp}\{\sum_{i=0}^{2}(Q_{1,i} - 2Q_{0,i}) + \sum_{i=2}^{4}(i-2)P_i^*\}R_{r,0} \quad (10)$$

$$\frac{dP_{r,1}}{dt} = -P_{r,1}\left[\frac{1}{\theta} + \{(r-2)k_{fp} + (1-\alpha)k_{AF}\}Y_0\right] + k_{td}R_{r,1}Y_0 + k_{tc}\sum_{s<r}(R_{s,0} + R_s^*)R_{r-s,1} + (1-\alpha)\sum_{i=1}^{3}k'_{Bi}R_{r+i,0} + k_{fp}\{\sum_{i=0}^{2}(Q_{1,i} - 2Q_{0,i}) + \sum_{i=2}^{4}(i-2)P_i^*\}R_{r,1} + k_{fp}Y_0\left\{\sum_{s=1}^{\infty}P_{r+s,0} + \frac{1}{2}\sum_{s=1}^{\infty}(P_{r+s,1} + P_{r+s}^*)\right) + (1-\alpha)k_{AF}(\sum_{i=1}^{2} iQ_{0,i} + \sum_{i=2}^{4}P_i^*)R_{r-1,0} \quad (11)$$

$$\frac{dP_{r,2}}{dt} = -P_{r,2}\left[\frac{1}{\theta} + \{(r-2)k_{fp} + 2(1-\alpha)k_{AF}\}Y_0\right] + \frac{k_{tc}}{2}(\sum_{s<r}R_{s,1}R_{r-s,1}) + (1-\alpha)\,k_{AF}(\sum_{i=1}^{2} iQ_{0,i} + \sum_{i=2}^{4}P_i^*)R_{r-1,1} + (1-\alpha)\sum_{i=1}^{3}k'_{Bi}R_{r+i,1} + k_{fp}Y_0\left\{\sum_{s=1}^{\infty}P_{r+s,2} + \frac{1}{2}\sum_{s=1}^{\infty}(P_{r+s,1} + P_{r+s}^*)\right) \quad (12)$$

Polymeric Oligomers. Dimers, trimers and tetramers, denoted by P_2^*, P_3^*, and P_4^* are formed by backbiting to the third, fifth, and seventh carbon from the chain end via the k'_{B1}, k'_{B2}, and k'_{B3} reaction, respectively. These oligomers can also be formed when an oligomeric radical (R_i^*) reacts with a TDB through addition, followed by β-scission via the $k_{\beta S2}$ reaction. These reactions, together with chain transfer to polymer and addition to a growing radical, which consume these oligomers, are summarized in Table 2. The mass balances for these oligomers, with reference to a transient CSTR, are given by

$$\frac{dP_2^*}{dt} = -P_2^*\left[\frac{1}{\theta} + (1-\alpha)k_{AF}Y_0\right] + \alpha k'_{B1}\left(Y_0 - \sum_{j=1}^{2}(R_{j,0} + R_{j,1} + R_j^*)\right) + (1-\alpha)k_{AF}R_1^*\left(\sum_{i=1}^{2} iQ_{0,i} + \sum_{i=2}^{4}P_i^*\right) \quad (13)$$

$$\frac{dP_3^*}{dt} = -P_3^*\left[\frac{1}{\theta} + \{(1-\alpha)k_{AF} + k_{fp}\}Y_0\right] + \alpha k'_{B2}\left(Y_0 - \sum_{j=1}^{3}(R_{j,0} + R_{j,1} + R_j^*)\right) + (1-\alpha)k_{AF}R_2^*\left(\sum_{i=1}^{2} iQ_{0,i} + \sum_{i=2}^{4}P_i^*\right) \quad (14)$$

$$\frac{dP_4^*}{dt} = -P_4^*\left[\frac{1}{\theta} + \{(1-\alpha)k_{AF} + 2k_{fp}\}Y_0\right] + \alpha k'_{B3}\left(Y_0 - \sum_{j=1}^{4}(R_{j,0} + R_{j,1} + R_j^*)\right) + (1-\alpha)k_{AF}R_3^*\left(\sum_{i=1}^{2} iQ_{0,i} + \sum_{j=2}^{4}P_i^*\right) \quad (15)$$

Monomer Balance. Monomer is consumed through propagation and initiation, and produced by chain end β-scission (depropagation). Its net rate of consumption, in a transient CSTR, is given by

$$\frac{d[M]}{dt} = \left(\frac{[M]_f - [M]}{\theta}\right) - k_p Y_0[M] - k_I[M]^3 + k_{\beta SE}\left(Y_0 - R_1^* - R_{1,0} - R_{1,1}\right) \quad (16)$$

Note that all radicals are capable of chain end β-scission, except those of length 1.

Overall Radical Balance. Radicals are produced by thermal initiation and consumed by the bimolecular termination reactions. Using the QSSA, the overall concentration of radicals (Y_0) is given by

$$Y_0 = \left(\frac{R_I}{k_{td} + k_{tc}}\right)^{1/2} \quad (17)$$

where the rate of thermal initiation of styrene (R_I) is given by[3]

$$R_I = 2k_I[M]^3 \quad (18)$$

Model Parameter Estimation. The developed model is rather complex and includes various kinetic rate constants, each with a frequency factor and an activation energy, resulting in a total of 20 parameters that have to be obtained. To produce a reliable model we have minimized the number of parameters estimated by fitting directly the data collected in this work, which are summarized in Table 1 in part 1, by using whenever possible values obtained from independent literature sources. The overall parameter estimation strategy used was (i) fix those parameters for which reliable values are available in the literature, (ii) use a restricted set of the experimental runs in Table 1 in part 1 to fit the remaining kinetic parameters, and (iii) use the obtained set of parameter values to predict the remaining experimental runs, so as to assess the predictive capabilities of the model.

Table 3. Rate Constant Values for All Reactions in the Model

parameter	k_0 (L/mol/s or L²/mol²/s or 1/s)	E_A/R (K)	source k_0	source E_A/R
k_p	4.3×10^7	3910	17	17
k_I	6.3×10^5	13 810	1	3
k_{tc}	1.06×10^9	753	18	18
k_{td}	1.52×10^8	753	18	18
$k_{\beta SE}$	8.3×10^{11}	10 600	1	15
k'_{B1}	8.3×10^9	9250	*a*	1
k'_{B2}	2.3×10^{10}	9250	*a*	1
k'_{B3}	1.7×10^8	9250	*a*	1
k_{fp}	1.2×10^6	6240	*a*	15
k_{AF}	3.3×10^7	4680	*a*	15

[a] Parameter values estimated in this work

The obtained values of all kinetic parameters are summarized in Table 3, together with the corresponding literature source, and we now discuss them individually. The activation energies and frequency factors for propagation[17] (k_p) and terminations[18] (k_{tc} and k_{td}) were obtained from pulsed-laser experimentation. The activation energy for thermal initiation of styrene was obtained from the literature[3] while its frequency factor, together with the frequency factor for chain end β-scission, was obtained from monomer conversion data in the first part of this work.[1] The activation energies for chain transfer to polymer (k_{fp}), chain end β-scission ($k_{\beta SE}$) and addition to terminal double bonds (k_{AF}) were taken from Kruse et al.[15] They estimated them using the Evans−Polanyi[16] relationship, as applied to the degradation of polystyrene.

The kinetics of the backbiting/β-scission reaction was described by the overall rate constant k'_B defined by eq 18 in part 1, whose activation energy has been established to be 77.5 kJ/mol. This lumped activation energy includes contributions from the 1:3, 1:5, and 1:7 backbiting reactions and therefore the activation energy for each overall backbiting reaction (k'_{B1}, k'_{B2} and k'_{B3}) was set to this value.

The frequency factors for the three backbiting reactions (k'_{B1}, k'_{B2} and k'_{B3}), chain transfer to polymer (k_{fp}) and addition fragmentation (k_{AF}) were estimated using three of the experimental runs in Table 1 in part 1, and specifically those at 15 min residence time and temperature values equal to 288, 316, and 343 °C. The considered experimental data included the number- and weight-average molecular weights and the weight fractions of dimers (2,4-diphenyl-1-butene), trimers (2,4,6-triphenyl-1-hexene), and tetramers (2,4,6,8-tetraphenyl-1-octene). In addition, we have used the terminal double bond distribution data that will be reported in the next section and have been obtained from MALDI−TOF MS measurements reported elsewhere.[2] The complexity of the experimental data set to be fitted makes it difficult to define correctly an objective function to be minimized. The different data have different accuracy, and there-

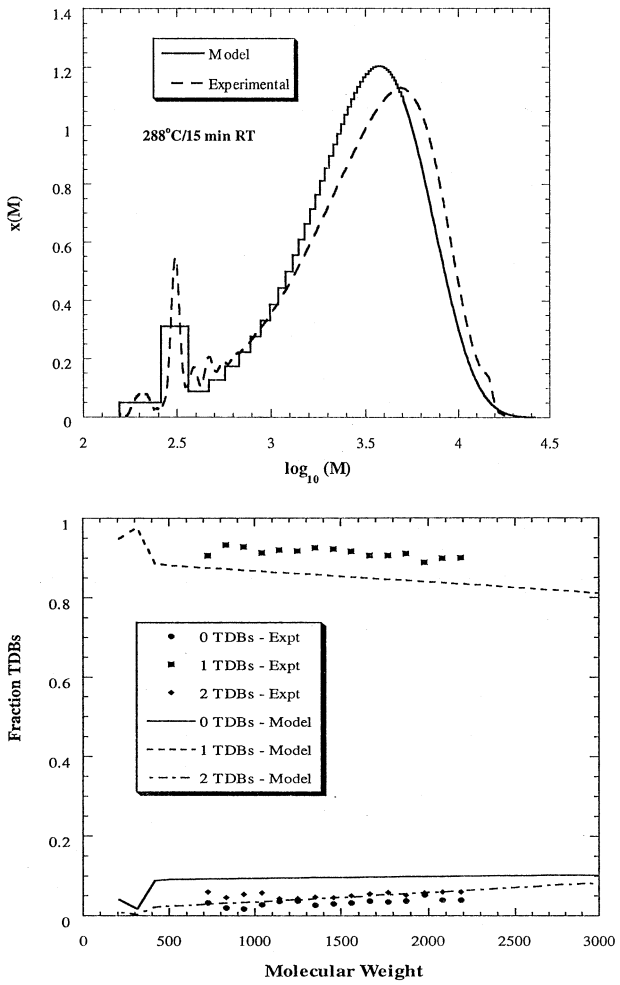

Figure 1. Model fitting comparison of the experimental (a) MWD and (b) TDB distributions at 288 °C and 15 min residence time.

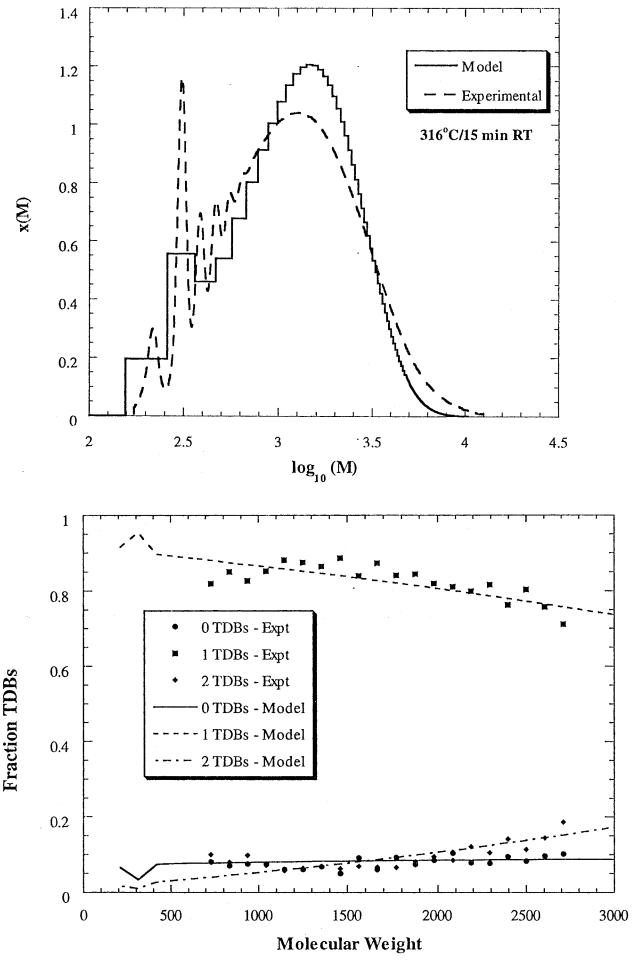

Figure 2. Model fitting comparison of the experimental (a) MWD and (b) TDB distributions at 316 °C and 15 min residence time.

fore, we are not in the position to properly weight them. Therefore, we performed only a manual fitting of the data based on a qualitiative evaluation of the agreement between calculated and experimental data. For the reliability of the obtained results, we count on the fact that the majority of the model parameters (including all the activation energies) have been taken from independent literature sources and that the values estimated for the five fitted frequency factors are within the range expected based on previous literature results.[14,15] It is worth noting that the number of parameters estimated is well balanced with the number of available experimental data, and, in addition the effect of the different parameters on the selected sets of experimental data is reasonably well decoupled, so that the correlation among the obtained estimates is expected to be modest. For example, the backbiting and chain transfer to polymer reactions have a similar effect on the average molecular weight, while their impact on the fraction of chains with 0, 1, or 2 TDBs and on the oligomer concentrations is significantly different. Conversely, the average molecular weight is relatively unaffected by the rate of addition/fragmentation, which mainly affects the concentration of oligomers.

To assess the reliability of the developed model, its results have been compared, without further adjustment of the kinetic parameters, to the remaining sets of experimental data reported in part 1. This comparison, together with that corresponding to the data that have been fitted, is discussed in the next section.

Model Results

Comparison with Experimental Data. Figures 1−3 show the experimental molecular weight and TDB distributions for the three experimental runs that have been used to fit the model parameters. These correspond to rows 5−7 in Table 1 in part 1, that is 15 min residence time and temperatures equal to 288, 316, and 343 °C, respectively. In the same figure, the model results obtained using the kinetic parameters in Table 3 are also shown. Note that we have plotted the model results in the form of a histogram, which corresponds to the fact mentioned above that the model computes each individual chain length. Accordingly, to judge about the agreement in the oligomer weight fractions, one should consider the area underneath the experimental GPC curves and the calculated histograms. It can be seen that the agreement for both TDB and molecular weight distributions is satisfactory for all three data sets. Specifically, the molecular weight calculations at 288 and 316 °C match the experimental data with less than 10% relative error, while the model overpredicts the molecular weight at 343 °C by less than 20%. Although the relative error for these data point seems high, it is worth noting that the absolute error is approximately 200 Da, corresponding to a difference in degree of polymerization of two monomer units. The

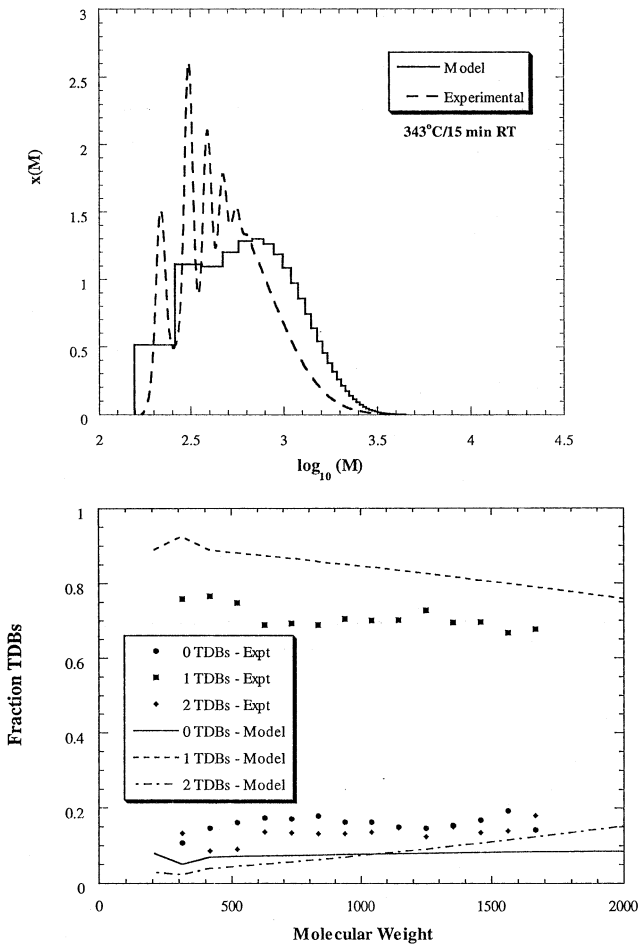

Figure 3. Model fitting comparison of the experimental (a) MWD and (b) TDB distributions at 343 °C and 15 min residence time.

agreement with the experimental fractions of TDBs is also satisfactory, as shown in Figures 1b, 2b and 3b, although some deviations appear again at 343 °C. On the whole we can say that the model is able to predict the trends in the end group distributions, and in particular the fact that there are significantly more chains with 1 than 0 or 2 TDBs.

As mentioned above, the parameters estimated from these three data sets were used to simulate the remaining experimental runs in order to test the predictive capabilities of the model. A detailed comparison with the experimental weight and number-average molecular weights and oligomer concentrations for all the considered experimental runs is summarized in Table 4. In Figures 4 and 5 the same comparison is shown in the conventional calculated vs experimental data plots. It can be seen that some deviation exists, particularly at the lowest molecular weights (which correspond to the highest temperatures); however, considering the broad range of experimental conditions, the predictive capabilities of the model are quite satisfactory.

Role of the Solvent. The effect of solvent concentration on the molecular weight distribution and oligomer concentrations has been discussed in part 1.[1] A reduction in the molecular weight and an increase in the concentration of oligomers were observed when increasing solvent concentration. These observations can be explained qualitatively by the reduction in the monomer concentration, which increases the probability of backbiting over propagation. A comparison between experimental and model predicted molecular weight distributions is shown in Figure 6, for the last two experiments listed in Table 1 in part 1, that is at 316 °C and 15 min residence time, with 10 and 25% *p*-xylene in the feed stream, respectively. Note that the experimental average molecular weights and concentrations of dimers, trimers, and tetramers are compared more in detail with the corresponding quantities predicted by the model in the last two rows of Table 4. The observed agreement confirms the reliability of the developed model in predicting the kinetic behavior of the system.

Sensitivity to the Kinetic Parameters. In the previous sections, we have developed a mechanistic model of the high temperature polymerization of styrene, which accounts in detail for the various involved chemical reactions. The considered kinetic scheme is indeed very rich, including several reactions that interact with each other in a complex way to eventually

Table 4. Comparison between Calculated and Experimental Values of the no. (M_n) and Weight (M_w) Molecular Weight Averages and the Weight Fractions of Dimers ($w_{P^*_2}$), Trimers ($w_{P^*_3}$) and Tetramers ($w_{P^*_4}$) for All Experimental Conditions Investigated

	model					experimental				
T (°C)/RT (min)	M_n	M_w	$w_{P^*_2}$	$w_{P^*_3}$	$w_{P^*_4}$	M_n	M_w	$w_{P^*_2}$	$w_{P^*_3}$	$w_{P^*_4}$
330/5	850	1544	0.030	0.083	0.038	825	1260	0.019	0.075	0.040
316/5	1181	2415	0.018	0.058	0.019	1112	2706	0.012	0.055	0.020
288/5	2463	6047	0.008	0.029	0.004	2754	7042	0.003	0.021	0.008
260/5	5517	15 260	0.003	0.014	0.001	5747	18 478			
343/15	492	700	0.085	0.160	0.123	422	571	0.114	0.191	0.141
316/15	824	1451	0.030	0.081	0.044	808	1548	0.026	0.076	0.047
288/15	1670	3652	0.011	0.038	0.010	1708	4047	0.011	0.035	0.013
260/15	3786	9661	0.005	0.018	0.002	3712	9567			
343/30	426	569	0.120	0.199	0.157	367	453	0.153	0.244	0.186
316/30	672	1082	0.042	0.102	0.069	615	1017	0.044	0.097	0.077
288/30	1308	2634	0.014	0.046	0.017	1280	2925	0.016	0.046	0.023
260/30	2955	7107	0.006	0.021	0.003	2656	5807			
343/60	377	481	0.166	0.234	0.182	315	371	0.267	0.318	0.167
316/60	562	838	0.061	0.129	0.100	512	720	0.071	0.130	0.110
288/60	1031	1908	0.019	0.057	0.029	963	2042	0.017	0.052	0.035
260/60	2297	5168	0.007	0.025	0.005	1769	3993			
343/90	354	442	0.198	0.253	0.190	309	351	0.276	0.335	0.172
316/90	500	708	0.078	0.115	0.126	464	641	0.065	0.142	0.137
260/90	1982	4284	0.008	0.028	0.007	1400	4021			
316/15[a]	797	1397	0.032	0.087	0.046	782	1428	0.026	0.081	0.047
316/15[b]	752	1306	0.036	0.097	0.050	682	1316	0.051	0.106	0.051

[a] Feed: 25% xylene/75% styrene. [b] Feed: 10% xylene/90% styrene.

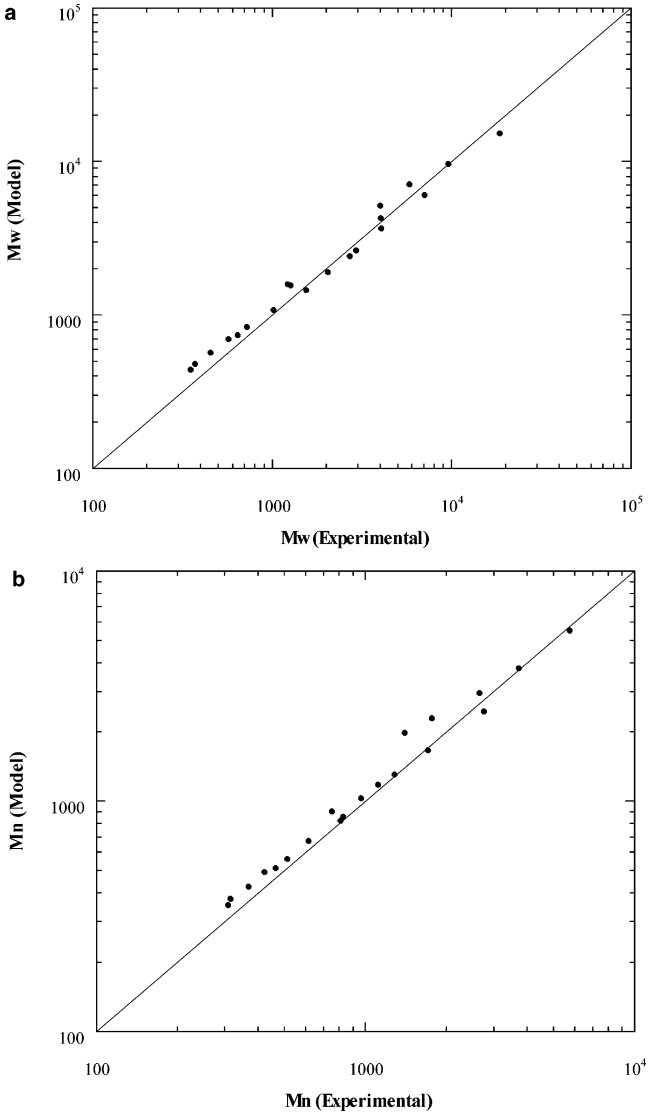

Figure 4. Calculated vs experimental (a) weight- and (b) number-average molecular weights for all experimental runs investigated.

determine the final polymer molecular weight and TDB distributions. The developed model offers the opportunity to quantitatively investigate these effects by analyzing the sensitivity of the molecular weight and end group behavior to changes in the various reaction rate constants.

The molecular weight and TDB distributions are determined by the relative importance of the various chain producing mechanisms, that is backbiting/β-scission, CTP/β-scission, addition/fragmentation, and termination. Since each reaction rate has a different activation energy and functional dependence, their relative importance is a function of the reaction conditions. It is useful to examine the ratio of each of these reaction rates relative to propagation as shown below:

$$\frac{R_{BB}}{R_p} = \frac{\sum_{i=1}^{3} k'_{Bi}}{k_p[M]}; \quad \frac{R_{CTP}}{R_p} = \frac{k_{fp}Q_1}{k_p[M]}; \quad \frac{R_{AF}}{R_p} = \frac{R_{AF}Q_0}{k_p[M]};$$

$$\frac{R_T}{R_p} = \frac{(k_{tc} + k_{td})[R^\bullet]}{k_p[M]}$$

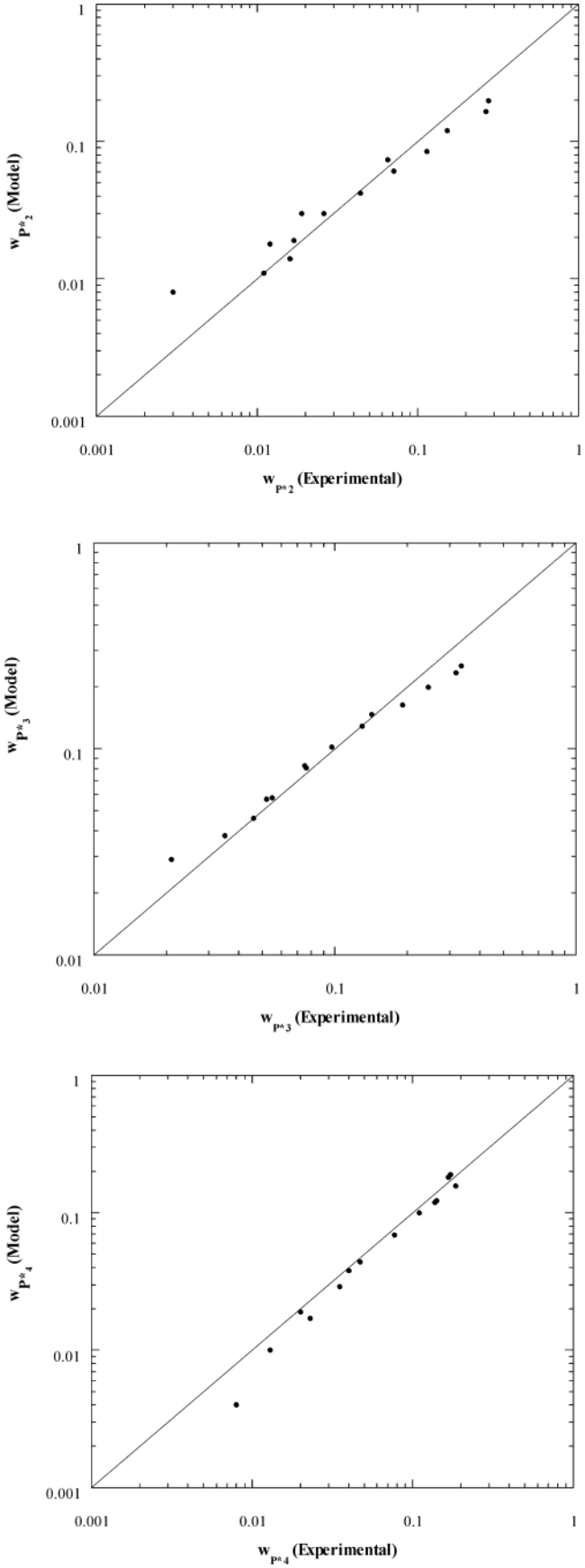

Figure 5. Calculated vs experimental weight fractions of dimers (a), trimers (b), and tetramers (c) for all experimental runs investigated.

where R_{BB}, R_{CTP}, R_{AF}, R_T, and R_p are the reaction rates for backbiting/β-scission, chain transfer to polymer/β-

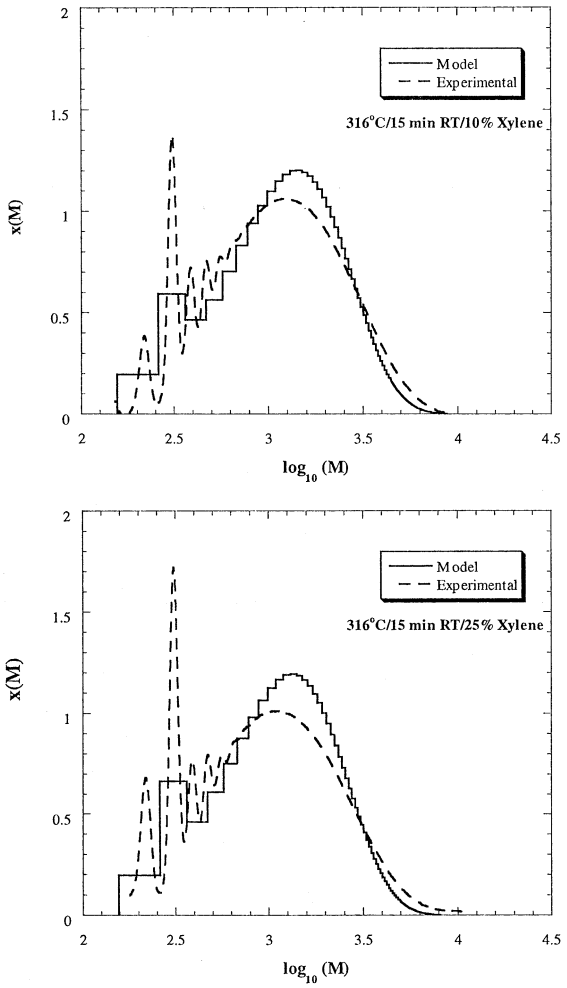

Figure 6. Comparison between calculated and experimental MWDs for the experimental runs at 316 °C, 15 min residence time, and 10% (a) or 25% (b) solvent in the feed stream.

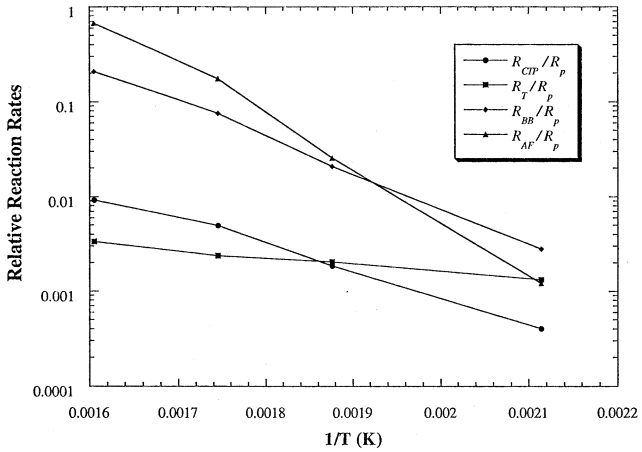

Figure 7. Model predictions of the rates of backbiting/β-scission, CTP/β-scission, addition/fragmentation, and bimolecular termination relative to propagation, as a function of temp.

scission, addition/fragmentation, termination and propagation, respectively. Each of these ratios represents the probability of a radical to undergo a specific chain production reaction with respect to that of adding a new monomer unit.

Figure 7 shows the values of each of the ratios above as a function of temperature, calculated at a 15 min residence time and using the model parameter values summarized in Table 1. It is somehow unexpected to see that the probability for the radical to undergo addition/fragmentation is clearly the largest. For increasing temperature values, the molecular weight decreases significantly, and the overall concentration of TDBs on polymer chains becomes so large to overtake that of unreacted monomer, resulting in the probability of addition/fragmentation to almost as high as that of propagation. The addition/fragmentation reaction has a slope higher than that of chain transfer to polymer and backbiting, even though its activation energy is lower. This is due to the fact that the rate of addition/fragmentation depends on the concentration of TDBs on polymer chains, which is also a strong function of temperature. It will be shown later that although the rate of AF is high, its impact on the molecular weight and TDB distribution is relatively small. Chain transfer to polymer is also significant; however, its overall rate is at least 1 order of magnitude lower than backbiting over the region of study. Termination becomes the dominant chain producing mechanism in the lower temperature region, (i.e., below 250 °C), where the polymerization begins to adopt the characteristics of a more traditional free radical polymerization.

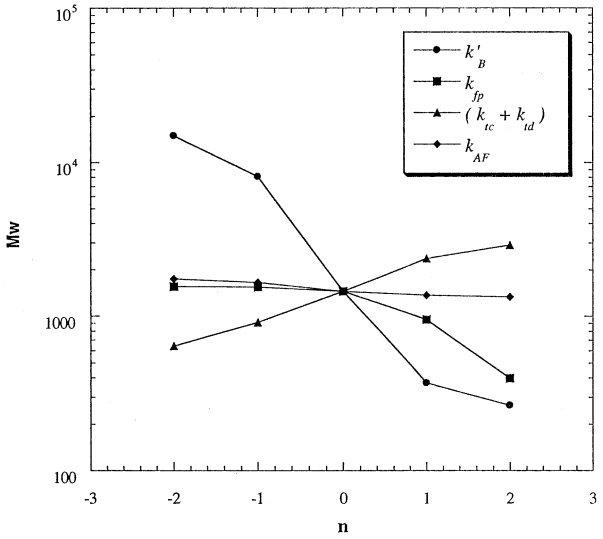

Figure 8. Model calculations of the average molecular weight obtained using the parameter values in Table 3, but changing one of the indicated rate constants at a time by a factor 10^n: (●) backbiting/β-scission, (■) CTP/β-scission, (◆) addition/fragmentation, and (▲) bimolecular termination

Each of the reactions above terminate the growing chain and thus limit its molecular weight, however due to their different kinetic characteristics, they have a different impact on the molecular weight and TDB distribution. This can be investigated using the developed model, by comparing the results obtained by changing each rate constant by ±2 orders of magnitude, while holding all the others constant and equal to the values reported in Table 1. The obtained results are shown in Figure 8 in terms of weight-average molecular weight for the reactions of backbiting/β-scission, CTP/β-scission, addition/fragmentation, and termination. It is clear that the backbiting reaction has the highest impact on the molecular weight.

Parts a and b of Figure 9 show the effect of backbiting/β-scission on the molecular weight and TDB distributions, respectively. As the rate of backbiting is increased, the molecular weight is continuously lowered, and the

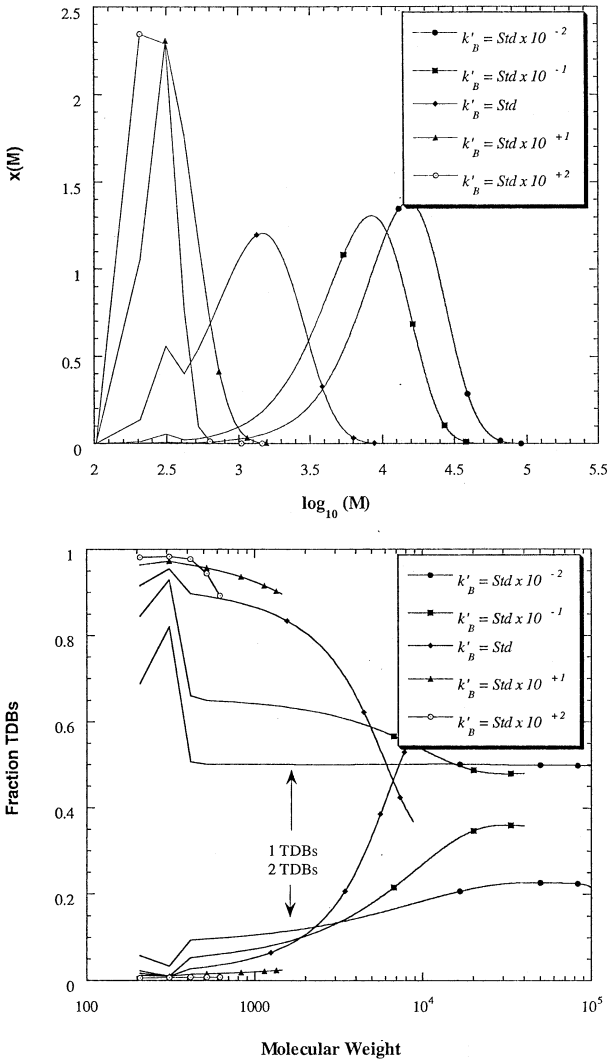

Figure 9. Effect of the backbiting/β-scission rate constant on the calculated (a) MWD and (b) TDB distribution, where the rate constant is varied ± 2 orders of magnitude from its standard value shown in Table 3.

concentration of oligomers increases until at the highest rate, predominantly oligomers of lengths 2, 3, and 4 are formed. Once backbiting occurs, the midchain radical either produces a polymeric oligomer and a growing radical smaller than the original radical, or a dead polymer chain and an oligomeric radical. In the former case, the growing radical is not terminated, only shortened by the characteristic length of the oligomer formed. This reduction in size of the growing radical is too small to be the main molecular weight reducing mechanism. In the latter case, the products of the backbiting/β-scission reaction are quite similar to those typical of chain transfer to a small molecule, whereby the growing chain is terminated and a small radical fragment is formed. It is indeed this second reaction that strongly affects on the molecular weight and makes backbiting/β-scission the reaction controlling the average molecular weight. Figure 9b shows the concentration of chains with 1 or 2 TDBs as a function of the molecular weight. It is seen that for the largest values of R_{BB}, where backbiting dominates over CTP, the most likely outcome is the production of chains with 1 TDB, since most radical chains have 0 TDBs. Conversely, as the rate of backbiting is lowered and CTP competes in producing

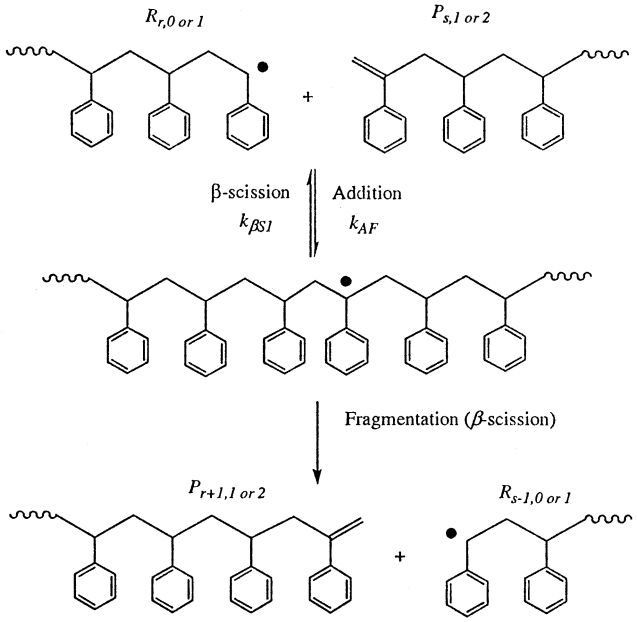

Figure 10. Addition/fragmentation mechanism.

chains, the number of chains with 2 TDB increases significantly at the expense of chains with 1 TDB.

Of particular interest are the results shown in Figure 8 for the addition/fragmentation reaction. It is seen that although we have seen in Figure 7 that this reaction is the fastest, it has practically no effect on the average molecular weight. This can be understood by examination of the reaction mechanism for addition/fragmentation, shown in Figure 10. The net result of this reaction is that the growing radical transfers to another chain, however in contrast to backbiting, the newly formed radical does not have to be smaller than the original one. Therefore, since the size of the radical produced depends solely on the size of the polymer chain that the original radical reacted with, the radical produced could be either larger or smaller than the original, making the overall effect on the average molecular weight negligible. This is a consequence of the polymer and radical chain length distributions being similar in size. Therefore, regardless of how fast this reaction is, it tends to redistribute radicals to polymers of similar size, leading to a largely ineffectual impact on the average molecular weight. This is not to say that there is no impact on the molecular weight distribution, although this also remains minor in comparison to backbiting, as we can see in Figure 11, parts a and b, where the molecular weight and TDB distributions for various values of R_{AF} are shown. In particular, we see that the concentration of oligomers changes significantly, due to their high concentration and thus high rate of consumption by addition, since the average molecular weight remains substantially constant, this leads to some changes in the shape of the molecular weight distribution. The effect on the TDB distribution is also minimal since the concentration of TDBs is conserved in this reaction.

At first glance, the effect of the rate of bimolecular termination shown in Figure 8 which, in contrast to all other terminations, leads to larger average molecular weights is indeed surprising. This result can be understood by considering that in this system the chain length is controlled by backbiting/β-scission and not by bimolecular termination, even when the termination rate

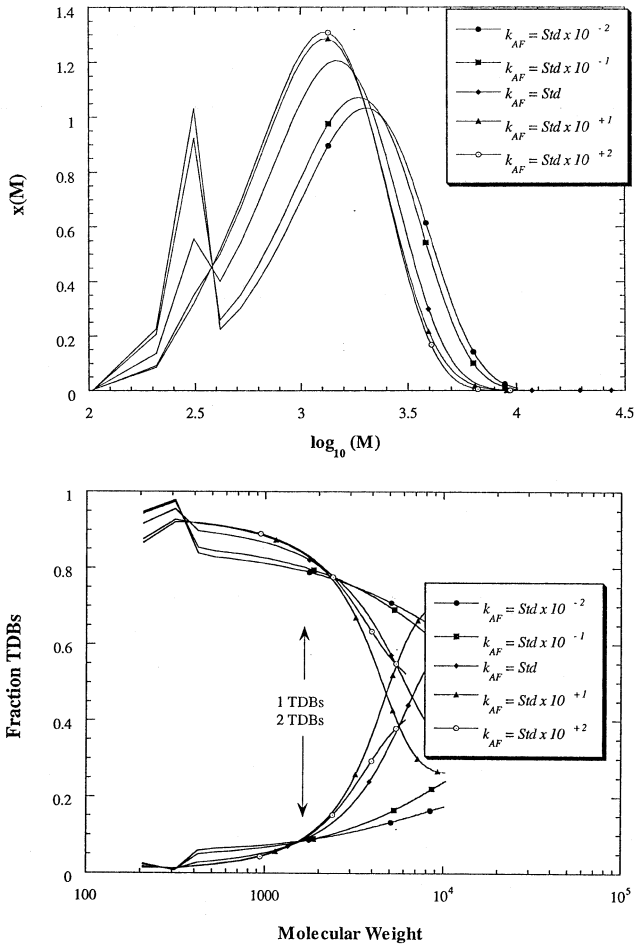

Figure 11. Effect of the addition/fragmentation rate constant on the calculated (a) MWD and (b) TDB distribution, where the rate constant is varied ±2 orders of magnitude from its standard value shown in Table 3.

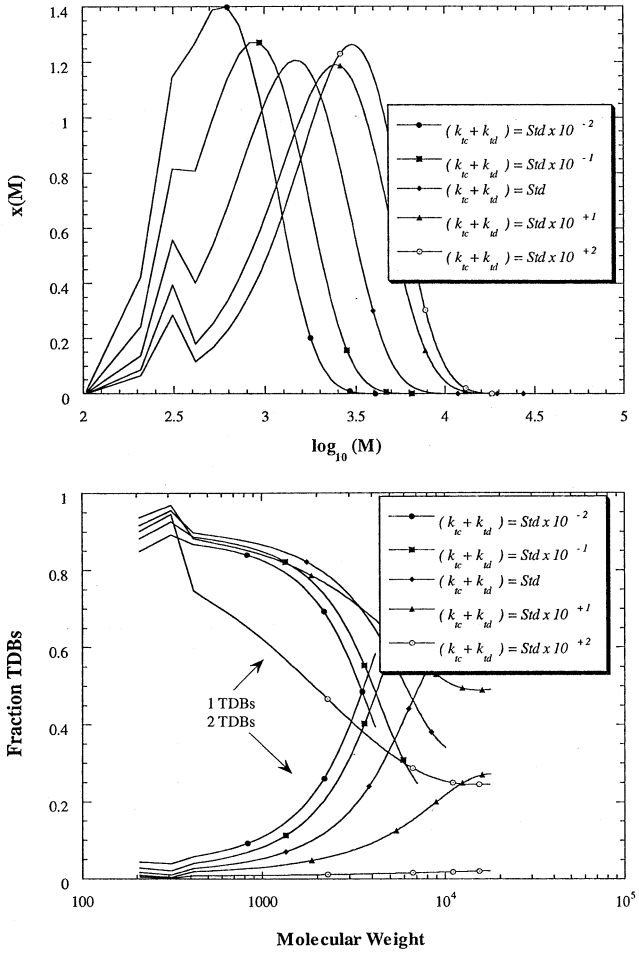

Figure 12. Effect of the bimolecular termination rate constant on the calculated (a) MWD and (b) TDB distribution, where the rate constant is varied ±2 orders of magnitude from its standard value shown in Table 3.

constant is increased 2 orders of magnitude above the standard value. When termination is increased, the concentration of radicals decreases, thus raising the concentration of monomer. This in turn raises the ratio of propagation to backbiting, and consequently the molecular weight, as shown in Figure 12a. The TDB distribution is also significantly affected by the rate of bimolecular termination, as shown in Figure 12b. It can be seen that at very high rates of bimolecular termination, the fraction of polymer chains with 0 TDBs increases significantly. This can be understood by realizing that the majority of radicals have 0 TDBs, and increasing the rate of bimolecular termination consequently raises the concentration of polymer chains with 0 TDBs.

Figure 8 shows that the effect of CTP/β-scission on molecular weight becomes significant only when the corresponding rate constant is larger than that of backbiting/β-scission. By comparing R_{BB} and R_{fp} we see that for the system under examination these two rates become in fact equal for an "n" value of 1.3 for k_{fp}, as shown in Figure 8. So for smaller values of k_{fp}, as shown in Figure 13a, CTP/β-scission has a very small effect on the molecular weight distribution since this is dominated by backbiting/β-scission. Only at larger values of k_{fp} does CTP/β-scission become dominating, and in fact the average molecular weight reduces significantly. The TDB distribution is strongly altered by CTP, as shown in Figure 13b. Since CTP is the necessary step to produce chains with 2 TDBs, increasing its rate increases the concentration of chains with 2 TDBs as shown in Figure 13b. In addition, since the reaction is chain length dependent, the longer chains have a greater probability of having a hydrogen abstracted, and therefore the concentration of 2 TDBs increases at higher chain lengths, as can be seen from Figure 13b.

Conclusions

In this work, we have developed a comprehensive kinetic model for the thermal polymerization of styrene at temperature values between 250 °C and 350 °C. The model describes the specific reactions that are known to be important at these reaction conditions, including polymerization, thermal initiation and degradation. The degradation routes include backbiting, chain transfer to polymer and addition to terminal unsaturation, all followed by β-scission. All activation energies for the rate parameters were taken from independent literature sources, with the exception of backbiting for which the experimental data obtained in part 1 of this work[1] have been used. The frequency factors for the degradation parameters were estimated by fitting the experimental molecular weight and TDB distribution data at three different temperature values, but under otherwise identical operating conditions. Although CTP and backbiting have similar effects on the molecular weight, their

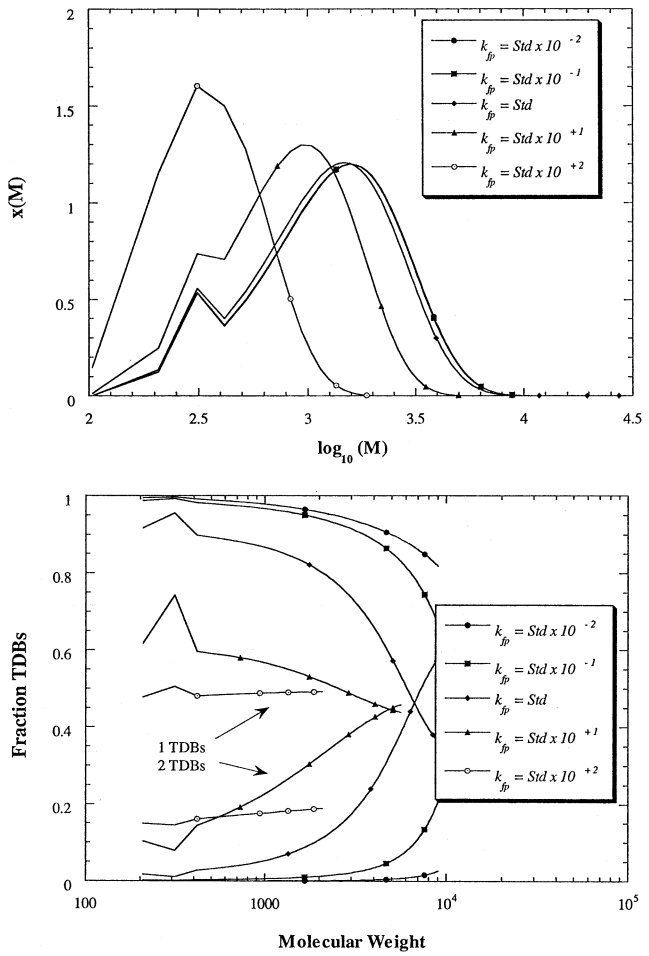

Figure 13. Effect of the CTP rate constant on the calculated (a) MWD and (b) TDB distribution, where the rate constant is varied ±2 orders of magnitude from its standard value shown in Table 3

impact on the TDB distribution is significantly different, allowing for relatively uncorrelated estimates of the corresponding frequency factors. Using these parameter values, the model was found to adequately predict the oligomer concentrations and the molecular weight distributions over the entire range of experimental conditions investigated in part 1, although it consistently over predicted the molecular weights at the highest temperature conditions. The operating conditions investigated include temperature values between 250 and 350 °C, residence time in the CSTR from 5 to 90 min and solvent concentrations in the feed stream up to 25%.

The developed kinetic model indicates that this polymerization is characterized and controlled by aggressive chain transfer reactions, including backbiting, chain transfer to polymer and addition to terminal double bonds. In each case a midchain radical is formed that subsequently undergoes β-scission degradation. It has been shown that these reactions, and specifically backbiting, control the molecular weight and TDB distributions. Bimolecular termination has been shown to play a rather minor role.

The model sensitivity to the kinetic parameters of the chain transfer reactions was studied, showing the specific and in some cases subtle differences in how each of these affects the polymerization. Addition/fragmentation, despite having the highest rate, has the least impact on the molecular weight and TDB distributions, while backbiting and to a lesser extent CTP, play the major roles.

Notation

Chemical Species

$R_{r,a}$ = radicals of length r with a terminal double bonds, $a = 0, 1$
$P_{r,a}$ = dead polymer of length r with a terminal double bonds, $a = 0, 1, 2$
$R^{\oplus}_{r,a}$ = midchain radicals of length r with a terminal double bonds
$R_{r,a}{}^{-i}$ = nonterminal radicals (produced through backbiting) of length "r" with "a" terminal double bonds and the radical located on the ith carbon from the chain end, $i = 3, 5, 7$
P^*_i = oligomeric polymers produced by characteristic β-scission and containing i monomer units, $i = 2, 3, 4$; $P^*_i = 0$ for $i > 4$
R^*_i = oligomeric radicals produced by characteristic β-scission and containing i monomer units, $i = 1, 2, 3$; $R^*_i = 0$ for $i > 3$
[M] = monomer concentration (mol/L)
$[M]_f$ = monomer concentration in the feed (mol/L)

Rate Constants

k_p = propagation rate constant
k_{tc}, k_{td} = termination rate constant (combination, disproportionation)
k_{fp} = chain transfer to polymer rate constant
k_I = initiation rate constant (thermal, chemical)
k_{B1}, k_{B2}, k_{B3} = backbiting rate constants (1:3, 1:5, 1:7 transfer)
k_{-B1}, k_{-B2}, k_{-B3}, = reverse backbiting rate constants (1:3, 1:5, 1:7 transfer)
k'_{B1}, k'_{B2}, k'_{B3} = backbiting/β-scission lumped rate constants (1:3, 1:5, 1:7 transfer)
k'_B = overall backbiting/β-scission lumped rate constant, $k'_{B1} + k'_{B2} + k'_{B3}$
k_B = overall backbiting rate constant, $k_{B1} + k_{B2} + k_{B3}$
k_{AF} = addition/fragmentation rate constant
$k_{\beta SE}$ = chain end β-scission rate constant (depropagation)
$k_{\beta S}$ = overall β-scission rate constant, $k_{\beta S1} + k_{\beta S2}$
$k_{\beta S1}$ = β-scission rate constant where the chain breaks in the first position
$k_{\beta S2}$ = β-scission rate constant where the chain breaks in the second position

Moments

Y_0 = overall zeroth-order moment of the radical distribution, equal to the total concentration of radicals (mol/L)
$Q_{i,a}$ = ith moment of the polymer distribution with "a" terminal double bonds
Q_i = Overall ith moment of the polymer distribution

Miscellaneous

α = probability that a midchain radical undergoes β-scission in the first position
τ = dimensionless quantity reflecting the ratio of the rate of disproportionation to propagation
β = dimensionless quantity reflecting the ratio of the rate of combination to propagation
$C_{fp} = k_{fp}/k_p[M]$
$C_{AF} = k_{AF}/k_p[M]$
$C_B = \sum_{j=1}^{3} k'_{Bi}/k_p[M]$
$C_s = k_{\beta SE}/k_p[M]$
R_I = rate of initiation (mol/L/min)
R_{AF} = rate of addition of radicals to TDB ((mol/L)/min)
R_p = rate of monomer propagation ((mol/L)/min)
R_{BB} = rate of backbiting/β-scission ((mol/L)/min)
R_{CTP} = rate of chain transfer to polymer ((mol/L)/min)
R_T = rate of bimolecular termination ()mol/L)/min)
θ = reactor residence time (min)

M_m = monomer molecular weight (Da)
M_n = number-average molecular weight
M_w = weight-average molecular weight
M_i = oligomer molecular weight, with "i" monomer units (Da)
w_{P_i}* = weight fraction of oligomer with "i" monomer units
$\delta(r - i)$ = function equal to 0 for $r \neq i$ and to 1 for $r = i$
$\delta(r > i)$ = function equal to 0 for $r \leq i$ and to 1 for $r > i$

References and Notes

(1) Campbell, J. D.; Morbidelli, M.; Teymour, F. *Macromolecules* **2003**, *36*, 5491.
(2) Campbell, J. D. Ph.D. Thesis, Swiss Federal Institute of Technology, ETH Zurich, 2003.
(3) Hui, A.; Hamielec, A. E. *J. Appl. Polym. Sci.* **1972**, *16*, 749.
(4) Hussain, A.; Hamielec, A. E. *J. Appl. Polym. Sci.* **1978**, *22*, 1207.
(5) Mayo, F. R. *J. Am. Chem. Soc.* **1968**, *90*, 1289.
(6) Hamielec, A. E.; MacGregor, J. F.; Webb, S.; Spychaj, T. In *Polymer Reaction Engineering*; Reichert, K. H., Geisler, W., Eds.; Hüthig and Wepf: New York, 1986; p 185.
(7) Ziff, R. M.; McGrady, E. D. *Macromolecules* **1986**, *19*, 2513.
(8) Wang, M.; Smith, J. M.; McCoy, B. J. *AIChE J.* **1995**, *41*, 1521.
(9) Kodera, Y.; McCoy, B. J. *AIChE J.* **1997**, *42*, 3205.
(10) McCoy, B. J.; Madras, G. *AIChE J.* **1997**, *43*, 802.
(11) Madras, G.; Smith, J. M.; McCoy, B. J. *Ind. Eng. Chem. Res.* **1995**, *34*, 4222.
(12) Madras, G.; Smith, J. M.; McCoy, B. J. *Ind. Eng. Chem. Res.* **1996**, *35*, 1795.
(13) McCoy, B. J. *AIChE J.* **1993**, *39*, 1827.
(14) Woo, O. S.; Broadbelt, L. *Catal. Today* **1998**, *40*, 121.
(15) Kruse, T. M.; Woo, O. S.; Broadbelt, L. J. *Chem. Eng. Sci.* **2001**, *56*, 971.
(16) 6) Evans, M. G.; Polanyi, M. T. *Faraday Soc.* **1938**, *34*, 11.
(17) Buback, M.; Gilbert, R. G.; Hutchinson, R.; Klumperman, B.; Kuchta, F. D.; Manders, B. B.; O'Driscoll, K. F.; Russel, G. T.; Schweer, J. *Macromol. Chem. Phys.* **1995**, *196*, 3267.
(18) Buback, M., Kuchta, F. *Macromol. Chem. Phys.* **1997**, *198*, 1455.

MA020643U